

Magnetic properties of 2D topological insulators

Zewei Chen and Tai Kai Ng

Department of Physics, Hong Kong University of Science and Technology, Clear Water Bay, Hong Kong, China

The effects of Hubbard-type on-site interactions on the BHZ model is studied in this paper for model parameters appropriate for the HgTe/CdTe quantum well. Within a simple mean field theory we search for plausible magnetic instabilities in the model and find that the ground state becomes *ferromagnetic* when the interaction strength between electrons in hole orbital is strong enough. The result can be understood by an approximate mapping of the Hubbard-BHZ model to the one band Hubbard model. The same mapping suggests that the magnetic and/or other ordered phases are more likely to occur in large gap topological insulators whose occupations are close to 1/2 for both electron and hole orbital.

I. INTRODUCTION

Topological phases entered condensed matter physics as early as the Kosterlitz-Thouless (KT) transition, Quantum Spin Chains (QSC) and Integer Quantum Hall effect (IQHE)¹⁻⁴ and becomes a heated topic in physics with the discovery of topological insulators (TIs)^{5,6}, topological superconductors (TSs)⁷⁻⁹ and quantum anomalous hall effect (QAHE)¹⁰. The role of topology in the physics of non-interacting systems is now basically understood with the completion of topological classification¹¹⁻¹³. However, the role of topology in interacting systems are much more non-trivial and remains to be explored. In 1D system, the classification of TIs and TSs is shown to be changed by interaction^{14,15}. For example, it is well known that the topology of non-interacting TIs cannot be changed without closing the bulk gap. However, this is not true in interacting systems where a first order topological phase transition may occur without closing the bulk gap¹⁶. New topological phases protected by interaction are also predicted to exist at dimensions $d > 1$ ¹⁷⁻²⁰.

In this paper, we study the effects of interaction in 2D TIs. We note that there have been many efforts trying to studied TIs with both short range or Coulomb interaction. The electron and hole bands in InAs/GaSb Quantum Well which occupy separate electron and hole layers form a good platform to search for topological exciton formed by Coulomb interaction²¹⁻²³. The effects of Hubbard-type interaction in the Bernevig, Hughes and Zhang (BHZ) model⁶ (Hubbard-BHZ model) has also been studied by Miyakoshi *et al.*²⁴ where a topological phase with anti-ferromagnetic order is predicted. However, the parameters used in their study do not describe the corresponding TI material- HgTe/CdTe quantum well²⁵⁻²⁷. In this paper, we study the Hubbard-BHZ model with parameters appropriate for the HgTe/CdTe quantum well and search for plausible magnetic phases. We find a first order phase transition where the insulating TI phase becomes a ferromagnetic metal phase when the hole-hole interaction is strong enough. By mapping approximately the Hubbard-BHZ model to the one band Hubbard model, we explain the origin of the ferromagnetic phase and predict that more exotic phases will ap-

pear when the electron occupation is close to 1/2 for both electron and hole orbital.

II. MODEL AND METHOD

We consider the BHZ model with Hubbard-type interaction on a square lattice with two orbital $\{|E\sigma\rangle, |H\sigma\rangle\}$ per site. The system is described by a Hamiltonian $H_T = H_{BHZ} + H_U$, where $H_{BHZ} = T + H_0$ is the BHZ model with

$$H_0 = \sum_{\langle i,j \rangle, \sigma} \varepsilon_E C_{i,E,\sigma}^\dagger C_{i,E,\sigma} + \varepsilon_H C_{i,H,\sigma}^\dagger C_{i,H,\sigma} \quad (1a)$$

being the on-site energy term with ε_τ being the on-site energy for τ orbital and

$$T = \sum_{\langle i,j \rangle, \sigma} t_E C_{i,E,\sigma}^\dagger C_{j,E,\sigma} + t_H C_{i,H,\sigma}^\dagger C_{j,H,\sigma} \quad (1b)$$

$$+ \sigma t_{EH} [i(C_{i,E,\sigma}^\dagger C_{i+\hat{x},H,\sigma} - C_{i,E,\sigma}^\dagger C_{i-\hat{x},H,\sigma})] \quad (1c)$$

$$+ (C_{i,E,\sigma}^\dagger C_{i+\hat{y},H,\sigma} - C_{i,E,\sigma}^\dagger C_{i-\hat{y},H,\sigma})] + c.c \quad (1d)$$

describes electron hopping between different lattice sites where t_τ, t_{EH} denotes intra-orbital and inter-orbital hopping, respectively. $C^\dagger(C)_{i,\tau,\sigma}$ creates/annihilates a τ -orbital ($\tau=E,H$) electron with spin $\sigma = \uparrow, \downarrow$ (or ± 1) on site i . $\langle i, j \rangle$ denotes nearest neighbor (NN) sites and $c.c$ denotes the hermitian conjugate.

$$H_U = \sum_i \sum_{\tau=E,H} U_\tau n_{i,\tau,\uparrow} n_{i,\tau,\downarrow} + \sum_i \sum_{\sigma,\sigma'} U_{EH} n_{i,E,\sigma} n_{i,H,\sigma'} \quad (2)$$

where U_τ ($\tau = E, H$), $U_{EH} > 0$ describe repulsive interaction between electrons and $n_{i,\tau,\sigma} = C_{i,\tau,\sigma}^\dagger C_{i,\tau,\sigma}$. Fourier transforming, we obtain

$$H_{BHZ} = \sum_{\mathbf{k}} \Psi_{\mathbf{k}}^\dagger \begin{pmatrix} h(\mathbf{k}) & 0 \\ 0 & h^*(-\mathbf{k}) \end{pmatrix} \Psi_{\mathbf{k}} \quad (3)$$

$$h(\mathbf{k}) = \varepsilon_{\mathbf{k}} I_2 + d_\alpha(\mathbf{k}) \cdot \mathbf{s}^\alpha$$

where $\Psi_{\mathbf{k}} = \{C_{E,\mathbf{k},\uparrow}, C_{H,\mathbf{k},\uparrow}, C_{E,\mathbf{k},\downarrow}, C_{H,\mathbf{k},\downarrow}\}^T$, \mathbf{s}^α 's are Pauli matrices,

$$C_{\tau,\mathbf{k},\sigma} = \frac{1}{\sqrt{N}} \sum_i \exp(i\mathbf{k} \cdot \mathbf{R}_i) C_{i,\tau,\sigma} \quad (4)$$

where N is the total number of sites and

$$\begin{aligned}
\varepsilon_{\mathbf{k}} &= C - \frac{2D}{a^2}(2 - \cos(k_x) - \cos(k_y)) \\
d_{\alpha}(\mathbf{k}) &= \left[\frac{A}{a} \sin(k_x), -\frac{A}{a} \sin(k_y), M(\mathbf{k}) \right] \\
M(\mathbf{k}) &= M - \frac{2B}{a^2}(2 - \cos(k_x) - \cos(k_y)) \\
D &= (t_E + t_H)/2, B = (t_E - t_H)/2, A = 2t_{EH} \\
M &= \frac{\varepsilon_E - \varepsilon_H}{2} - 2(t_E - t_H) \\
C &= \frac{\varepsilon_E + \varepsilon_H}{2} - 2(t_E + t_H)
\end{aligned} \tag{5}$$

where a is the lattice constant. Expanding the Hamiltonian (3) around the Γ point $\mathbf{k} = \mathbf{0}$, we see that H reduces to the continuum BHZ Hamiltonian describing topological insulators⁶, with $-(D + (-)B)k^2$ being the kinetic term of the electron (E) and hole (H) orbital and M being the Dirac mass. The topological region is characterized by $M \cdot B > 0$. A describes the hybridization between the H and E orbital and C is a overall constant energy term which will be absorbed in the chemical potential in the following.

We shall treat the interaction term in a mean-field theory where

$$\begin{aligned}
n_{i,\tau,\sigma} n_{i\tau',\sigma'} &\approx \langle n_{i,\tau,\sigma} \rangle n_{i,\tau',\sigma'} + \langle n_{i,\tau',\sigma'} \rangle n_{i,\tau,\sigma} \\
&\quad - \langle n_{i,\tau,\sigma} \rangle \langle n_{i,\tau',\sigma'} \rangle
\end{aligned}$$

and the mean field Hamiltonian becomes,

$$H_{MF} = H_{BHZ} + \sum_{i,\sigma,\tau} (U_{\tau} \langle n_{i,\tau,-\sigma} \rangle + U_{EH} \langle n_{i,\bar{\tau}} \rangle) n_{i,\tau,\sigma} \tag{6}$$

where $\bar{E}(\bar{H}) = H(E)$ $n_{i,\tau} = \sum_{\sigma} n_{i,\tau,\sigma}$ and $\langle \dots \rangle$ denotes (ground state) expectation value.

To understand the physics behind the mean-field theory, we first consider the case when the hybridization between the E and H orbits vanishes. In this case the two bands overlap because of band inversion (see Fig.(1)) and a small part of the E-band is occupied whereas the H-band is almost filled (see Fig.(1(a))). In this case the E and H bands are described separately by single-band Hubbard models which are almost empty/filled. Mean-field studies for single band Hubbard model on square lattice has been carried out long time ago²⁸ and it was found that the ground state is *anti-ferromagnetic* at and close to half filling and becomes *ferromagnetic* away from half filling when the interaction strength U is large than certain critical value. In HgTe/CdTe quantum well the E and H bands are nearly empty or fully filled, correspond to the case in Fig.(1(a)), suggesting that we should look for ferromagnetic phases in our mean-field theory. Anti-ferromagnetic phase is expected only if the band inversion is so large that the two bands are both nearly half filled (case shown in Fig.(1(b))). We've searched for both *ferromagnetic* and *anti-ferromagnetic* phases numerically

in our study and find that the *antiferromagnetic* phase has higher energy for band parameters appropriate for HgTe/CdTe quantum well. In the following we shall focus on the *paramagnetic* and *ferromagnetic* phases.

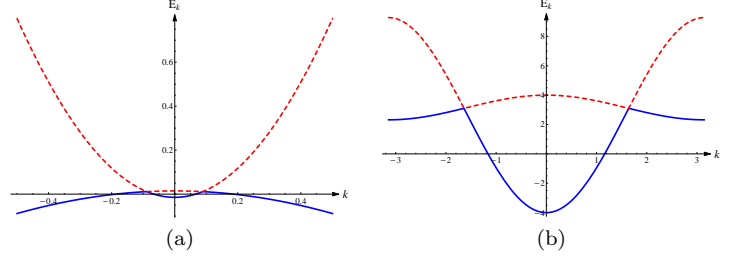


FIG. 1. Schematic band structure illustrating the filling of the E and H bands. The blue-solid/red-dash color denotes the part of bands which are occupied/empty. (a) The case for small band inversion corresponding to HgTe/CdTe quantum well. (b) The situation with large band inversion.

The mean field Hamiltonian which captures both *paramagnetic* and *ferromagnetic* phases is in k -space,

$$H_{MF} = H_{BHZ} + \sum_{\tau,\sigma} h_{\tau,\sigma} n_{\tau,\mathbf{k},\sigma} \tag{7}$$

$$h_{\tau,\sigma} = \frac{U_{\tau}}{2} (n_{\tau} - \sigma m_{\tau}) + U_{EH} n_{\bar{\tau}}$$

where n_{τ} and m_{τ} are the occupation number and the magnetization of the τ orbital, respectively with

$$\begin{aligned}
n(m)_{\tau} &= \frac{1}{V} \sum_{\mathbf{k}} \langle n_{\tau,\mathbf{k},\uparrow} \rangle + (-) \langle n_{\tau,\mathbf{k},\downarrow} \rangle \\
&= \frac{1}{V} \sum_{\mathbf{k}} (\Theta(\mu - E_{\mathbf{k},\uparrow,+}) |\alpha_{\tau,\mathbf{k},\uparrow}|^2 + \Theta(\mu - E_{\mathbf{k},\uparrow,-}) |\beta_{\tau,\mathbf{k},\uparrow}|^2 \\
&\quad + (-) (\Theta(\mu - E_{\mathbf{k},\downarrow,+}) |\alpha_{\tau,\mathbf{k},\downarrow}|^2 + \Theta(\mu - E_{\mathbf{k},\downarrow,-}) |\beta_{\tau,\mathbf{k},\downarrow}|^2) \\
|\alpha_{\tau,\mathbf{k},\sigma}|^2 &= \frac{1}{2} \left(1 + \frac{\text{Sign}_{\tau} M_{\mathbf{k}}}{\sqrt{(M_{\mathbf{k}} + \Sigma_{2\sigma})^2 + |A_{\mathbf{k}}|^2}} \right) \\
|\beta_{\tau,\mathbf{k},\sigma}|^2 &= \frac{1}{2} \left(1 - \frac{\text{Sign}_{\tau} M_{\mathbf{k}}}{\sqrt{(M_{\mathbf{k}} + \Sigma_{2\sigma})^2 + |A_{\mathbf{k}}|^2}} \right)
\end{aligned} \tag{8}$$

where $n_{\tau,\mathbf{k},\sigma} = C_{\tau,\mathbf{k},\sigma}^{\dagger} C_{\tau,\mathbf{k},\sigma}$ and $\text{Sign}_{E(H)} = 1(-1)$. $\Theta(x)$ is the step function. $E_{\mathbf{k},\sigma,\pm}$ is the eigen-energies of H_{MF} given by,

$$E_{\mathbf{k},\sigma,\pm} = \varepsilon_{\mathbf{k}} + \Sigma_{1\sigma} \pm \sqrt{(M_{\mathbf{k}} + \Sigma_{2\sigma})^2 + |A_{\mathbf{k}}|^2} \tag{9}$$

where,

$$\begin{aligned}
\Sigma_{1\sigma} &= \frac{U_E(n_E - \sigma m_E) + U_H(n_H - \sigma m_H) + 4U_{EH}}{4}, \\
\Sigma_{2\sigma} &= \frac{U_E(n_E - \sigma m_E) - U_H(n_H - \sigma m_H) + 2U_{EH}(n_H - n_E)}{4}, \\
A_{\mathbf{k}} &= \frac{A}{a} (\sin(k_x) + i \sin(k_y)).
\end{aligned} \tag{10}$$

The ground state energy density is,

$$\frac{E_g}{V} = \frac{1}{V} \sum_{\mathbf{k}} \sum_{i=\pi,\sigma} \Theta(\mu - E_{\mathbf{k},i}) E_{\mathbf{k},i} - \frac{U_E}{4} (n_E^2 - m_H^2) - \frac{U_H}{4} (n_H^2 - m_H^2) - U_{EH} n_E n_H. \quad (11)$$

The mean field parameters $n(m)_\tau$ are determined self-consistently *via* the mean-field equations.

III. RESULTS AND PHASE DIAGRAM

We consider the half filled case for the BHZ model where the chemical potential is in the gap and the system is a topological insulator. We employ the parameters appropriate for the 7.5nm HgTe/CdTe quantum well with $M = -0.0146\text{eV}$, $B = -1.87\text{eV} \cdot \text{nm}^2$, $A = 0.55\text{eV} \cdot \text{nm}$, $D = -1.45\text{eV} \cdot \text{nm}^2$ and $C = 0$.²⁹ The lattice constant a is chosen to be 1 nm.

In Fig.(2(a)) we show the self-consistent determined mean field parameters, n_H , m_E and m_H as a function of interaction strength U_H of the H orbital with (i) $U_E = U_{EH} = 0$, (ii) $U_E = 10\text{eV}, U_{EH} = 0$ and (iii) $U_E = 0, U_{EH} = 1.5\text{eV}$ respectively. We first consider the case with only $U_H \neq 0$ which is similar to the single band Hubbard model. We note that an important difference between the single band Hubbard model and the BHZ model is that in our case, the relative position of the two bands depends on interaction. When U_H increases, the on-site energy of H orbital is shifted upward while the E orbital energy remains stationary leading to increasing population in E band. Changing other interactions have similar effects. Thus we are actually moving along a curve in the density-interaction phase diagram of the one-band Hubbard model when interaction changes. At small U_H , only one solution with $m_H = 0$ is found. The system remains a TI. As interaction strength increase, two self-consistent solutions appear. The ground state is the one with lower energy. The energy difference between the *ferromagnetic* and *paramagnetic* phases are shown in Fig.(2(b)). We find a first order phase transition between *paramagnetic* and *ferromagnetic* phases indicated by the sign change of the energy difference between the two phases. We note that despite $U_E = 0$ in this case, m_E has non-vanishing negative value as long as $m_H \neq 0$ because of nonzero band hybridization $A \neq 0$.

Including U_E and U_{EH} have similar effect as U_H . U_E increases the energy of E orbital (see Fig.(3)). However, as discussed above, the occupation number of E orbital is much smaller than H, and the effect of U_E is much smaller compared to U_H because of smallness of n_E . Therefore U_E has almost no effect on the phase transition. U_{EH} raises the energies of the two orbital simultaneously but with different values depending on the occupation numbers of the two bands. The shift in energy of E(H) orbital is proportional to $n_H(n_E)$. Again, since $n_H \gg n_E$, the energy of E orbital is shifted faster than H orbital lead-

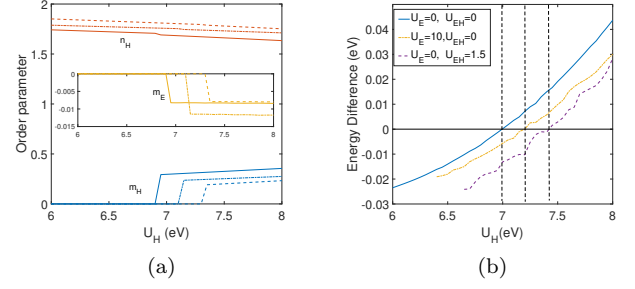


FIG. 2. (a). Order parameters n_H, m_H, m_E verse interaction strength U_H . Solid lines are for $U_E = 0, U_{EH} = 0$. Dash-dot lines are for $U_E = 10\text{eV}, U_{EH} = 0$. Dash lines are for $U_E = 0\text{eV}, U_{EH} = 1.5\text{ eV}$. (b) Energy difference between nonmagnetic phase (NM) and *ferromagnetic* phase (FM) $E_{NM} - E_{FM}$. Different styles of line represent same parameter in (a)

ing to decreasing/increasing occupation number in E/H orbital for $U_{EH} > 0$.

The dependence of the *paramagnetic-ferromagnetic* phase boundary on the interactions are summarized in the phase diagram in Fig.(4). we see that the ferromagnetic region shrink when $U_E, U_{EH} > 0$ since these interactions effectively increase/decrease the occupation of H/E orbital. We note that besides the *ferromagnetic* phase, we have also searched for the solution of *anti-ferromagnetic* phase. We find that the anti-ferromagnetic phase exists only if $U_H \gg U_E, U_{EH}$ such that the en-

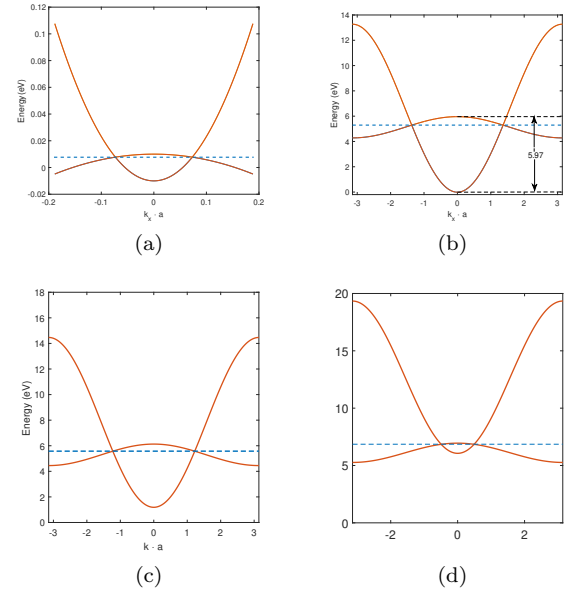


FIG. 3. Band structure assuming $A = 0$ (along $k_x \in [-\pi, \pi], k_y = 0$) evolution with interaction strength. (a) $U_H = U_E = U_{EH}$. The blue-dash line shows the chemical potential. (b) $U_H = 6.95\text{eV}, U_E = U_{EH} = 0$. (c) $U_H = 6.95\text{eV}, U_E = 10\text{eV}, U_{EH} = 0$. (d) $U_H = 6.95\text{eV}, U_E = 10\text{eV}, U_{EH} = 3\text{eV}$

ergy of H orbital is lifted to be close to the 1/2 filling case shown in Fig.(1(b)).

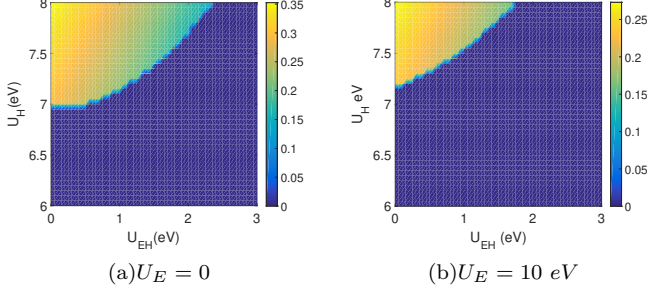


FIG. 4. Phase diagram in $U_H - U_{EH}$ space with given U_E . The color represent the magnitude of magnetization.

The evolution of the band structure in the two phases is shown in Fig.(5). The band structure without interaction is shown in Fig.(5(a)). In this case the bands are doubly degenerate with band extremum at Γ point. The band structure near the phase transition point ($U_H = 6.95\text{eV}$, $U_E = U_H = 0$) is shown in Fig.5(b). We see that the band extremum are shifted to finite k -points due to the upward shifting of H-orbital compared with the E-orbital. The band degeneracy is lifted by the magnetization and the system becomes gapless in the *ferromagnetic* phase (Fig.5(c)). We caution that the E and H orbital are linear combination of different atomic orbital (s and p orbitals) in realistic material. Although a state with uniform magnetization is obtained in the lattice model, the magnetization distribution on the two atomic orbital are in general different in real materials.

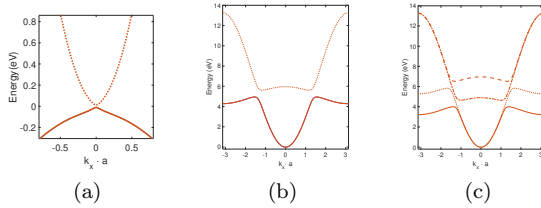


FIG. 5. Band structure (along $k_x \in [-\pi, \pi], k_y = 0$) evolution with interaction strength U_H .

IV. SUMMARY AND DISCUSSIONS

Summarizing, we studied in this paper the effects of Hubbard-type on-site interaction on the BHZ model. Within a mean-field theory, we find a ferromagnetic state when U_H is large enough and the band inversion is small. The system becomes *gapless* (metallic) in the ferromagnetic phase. We have computed the Chern number (C) for the energy bands in the ferromagnetic phase and find that they have values $C = \pm 1$, i.e., the ferromagnetic transition is *not* a topological phase transition.

Our result is qualitatively consistent with the phase diagram inferred from Ref.[28] for the single-band Hubbard model. The magnitude of U_H is roughly 7 eV close to the critical point and is about a quarter of the band width, which is not unrealistic. It should be emphasized that mean field approximation has overestimated the tendency of *ferromagnetic* ordering. The region of *ferromagnetic* phase shrinks when more accurate calculations are performed on the one-band Hubbard model^{30,31} and similar result is expected here. We note that more exotic phases are proposed to appear in the one band Hubbard model when the system is close to half-filling³²⁻⁴⁶ and similar situation is expected here when the H-orbital is lifted up further such that both E- and H- orbital are close to half-filling. The parameters we use in this paper are base on 7.5nm HgTe/CdTe quantum well.

Our result may be generalized to other similar 2DTI material; for example, the InAs/GaSb quantum well. Due to the inversion symmetry breaking, InAs/GaSb quantum well has considerable Rashba spin orbit coupling and is described by a modified BHZ model on square lattice with extra (small) bulk inversion asymmetry (BIA) and structural inversion asymmetry (SIA) term described by the tight-binding Hamiltonian $H_{TB} = H_{BHZ} + H_{BIA} + H_{SIA}$, where

$$H_{BIA} = \sum_{\mathbf{k}, \tau} \Delta_E(\mathbf{k}) C_{E,\mathbf{k},\uparrow}^\dagger C_{E,\mathbf{k},\downarrow} + \Delta_H(\mathbf{k}) C_{H,\mathbf{k},\uparrow}^\dagger C_{H,\mathbf{k},\downarrow} + \Delta_0(C_{E,\mathbf{k},\uparrow}^\dagger C_{H,\mathbf{k},\downarrow} - C_{H,\mathbf{k},\uparrow}^\dagger C_{E,\mathbf{k},\downarrow}) + c.c. \quad (12)$$

$$H_{SIA} = \sum_{\mathbf{k}} i\xi_E(\mathbf{k}) C_{E,\mathbf{k},\uparrow}^\dagger C_{E,\mathbf{k},\downarrow} + c.c.$$

where $\Delta_{E(H)}(\mathbf{k}) \rightarrow \Delta_{E(H)}k_{+(-)}$, $\xi_E(\mathbf{k}) \rightarrow \xi_E k_-$ in the $\mathbf{k} \rightarrow 0$ limit. ξ_E is the electron Rashba term where $k_{\pm} = k_x \pm ik_y$. This leads to spin-flip term in the Hamiltonian H_{TB} . However, the interaction term is of the same form as the H_U and the Hamiltonian has the same form as H_T after diagonalizing H_{TB} except that the spins have different quantization axis at each \mathbf{k} point. In particular, the Hubbard interaction has similar effect on the model as the original Hubbard-BHZ model and the effect of orbital filling will be similar.

As discussed above, we see that when the H-orbital is lifted up and the system becomes a large gap topological insulator, stronger effects of electron interaction (and more exotic phases) are expected when the orbital are close to half-filling. The search for large gap topological insulator has been a hot topic after the discovery of topological insulator since larger gap implies that the topological effects can be measured at higher temperatures. This is important for the application of TI based electronic devices. Our calculation suggests that large gap TI is also helpful to realize exotic phases in TI. We note that large gap 2DTI has been predicted to exist in transition metal dichalcogenides⁴⁷ described by the $\mathbf{k} \cdot \mathbf{p}$

Hamiltonian,

$$H_{TMD} = \begin{pmatrix} E_p(k_x, k_y) & 0 & -iv_1\hbar k_x & v_2\hbar k_y \\ 0 & E_p(k_x, k_y) & v_2\hbar k_y & -v_1\hbar k_x \\ iv_1\hbar k_x & v_2\hbar k_y & E_d(k_x, k_y) & 0 \\ v_2\hbar k_y & iv_1\hbar k_x & 0 & E_d(k_x, k_y) \end{pmatrix} \quad (13)$$

in the basis of p and d orbital where $E_p = -\delta + \frac{\hbar^2 k_x^2}{2m_x^p} + \frac{\hbar^2 k_y^2}{2m_y^p}$, $E_d = \delta + \frac{\hbar^2 k_x^2}{2m_x^d} + \frac{\hbar^2 k_y^2}{2m_y^d}$. δ is the inverted gap with value ranges from 0.284 eV to 0.978 eV (calculated in GW approximation)⁴⁷. The inverted gaps are 20 to 100

times of HgTe/CdTe and InAs/GaSb quantum wells leading to closer to half band fillings for both p and d orbital. There has been some experimental evidence indicating that the 1T' structure of TMD material WTe₂ is a 2D topological insulator^{48,49}. Our study suggests that this material may be a good candidate for strong correlation effect.

V. ACKNOWLEDGEMENT

This work is supported by Hong Kong RGC through grant HKUST3/CRF/13G.

-
- ¹ J. M. Kosterlitz and D. J. Thouless, Journal of Physics C: Solid State Physics **6**, 1181 (1973).
 - ² F. Haldane, Physics Letters A **93**, 464 (1983).
 - ³ K. v. Klitzing, G. Dorda, and M. Pepper, Phys. Rev. Lett. **45**, 494 (1980).
 - ⁴ Y. Hatsugai, Journal of Physics: Condensed Matter **9**, 2507 (1997).
 - ⁵ X.-L. Qi and S.-C. Zhang, Rev. Mod. Phys. **83**, 1057 (2011).
 - ⁶ B. A. Bernevig, T. L. Hughes, and S.-C. Zhang, Science **314**, 1757 (2006).
 - ⁷ A. Y. Kitaev, Physics-Uspekhi **44**, 131 (2001).
 - ⁸ L. Fu and C. L. Kane, Phys. Rev. Lett. **100**, 096407 (2008).
 - ⁹ C. L. M. Wong and K. T. Law, Phys. Rev. B **86**, 184516 (2012).
 - ¹⁰ C.-Z. Chang *et al.*, Science **340**, 167 (2013).
 - ¹¹ A. P. Schnyder, S. Ryu, A. Furusaki, and A. W. W. Ludwig, Phys. Rev. B **78**, 195125 (2008).
 - ¹² A. Kitaev, AIP Conference Proceedings **1134** (2009).
 - ¹³ S. Ryu, A. P. Schnyder, A. Furusaki, and A. W. W. Ludwig, New Journal of Physics **12**, 065010 (2010).
 - ¹⁴ L. Fidkowski and A. Kitaev, Phys. Rev. B **83**, 075103 (2011).
 - ¹⁵ L. Fidkowski and A. Kitaev, Physical Review B **81**, 134509 (2010).
 - ¹⁶ A. Amaricci, J. C. Budich, M. Capone, B. Trauzettel, and G. Sangiovanni, Phys. Rev. Lett. **114**, 185701 (2015).
 - ¹⁷ R. A. Santos and D. B. Gutman, Phys. Rev. B **92**, 075135 (2015).
 - ¹⁸ J. Wen, A. Rüegg, C.-C. J. Wang, and G. A. Fiete, Phys. Rev. B **82**, 075125 (2010).
 - ¹⁹ C. N. Varney, K. Sun, M. Rigol, and V. Galitski, Phys. Rev. B **82**, 115125 (2010).
 - ²⁰ C. Wang, A. C. Potter, and T. Senthil, Science **343**, 629 (2014).
 - ²¹ B. Seradjeh, J. E. Moore, and M. Franz, Phys. Rev. Lett. **103**, 066402 (2009).
 - ²² D. Pikulin and T. Hyart, Phys. Rev. Lett. **112**, 176403 (2014).
 - ²³ J. C. Budich, B. Trauzettel, and P. Michetti, Phys. Rev. Lett. **112**, 146405 (2014).
 - ²⁴ S. Miyakoshi and Y. Ohta, Phys. Rev. B **87**, 195133 (2013).
 - ²⁵ M. König *et al.*, Science **318**, 766 (2007).
 - ²⁶ D. G. Rothe *et al.*, (2010), arXiv:1002.2904.
 - ²⁷ I. Knez and R.-R. Du, Frontiers of Physics **7**, 200 (2012).
 - ²⁸ J. E. Hirsch, Phys. Rev. B **31**, 4403 (1985).
 - ²⁹ W. Beugeling, C. X. Liu, E. G. Novik, L. W. Molenkamp, and C. Morais Smith, Phys. Rev. B **85**, 195304 (2012).
 - ³⁰ P. Fazekas, *Lecture Notes on Electron Correlation and Magnetism* (World Scientific, 1999).
 - ³¹ J. Kanamori, Progress of Theoretical Physics **30**, 275 (1963).
 - ³² T. A. Maier, M. Jarrell, T. C. Schulthess, P. R. C. Kent, and J. B. White, Phys. Rev. Lett. **95**, 237001 (2005).
 - ³³ E. Dagotto, Rev. Mod. Phys. **66**, 763 (1994).
 - ³⁴ C. J. Halboth and W. Metzner, Phys. Rev. Lett. **85**, 5162 (2000).
 - ³⁵ J. E. Hirsch and S. Tang, Phys. Rev. Lett. **62**, 591 (1989).
 - ³⁶ H. J. Schulz, EPL (Europhysics Letters) **4**, 609 (1987).
 - ³⁷ D. Yoshioka, *Slave-Fermion Mean Field Theory of the Hubbard Model* (Springer Berlin Heidelberg, Berlin, Heidelberg, 1989), pp. 124–131.
 - ³⁸ T. Baier, E. Bick, and C. Wetterich, Phys. Rev. B **70**, 125111 (2004).
 - ³⁹ A. Macridin, M. Jarrell, T. Maier, P. R. C. Kent, and E. D'Azevedo, Phys. Rev. Lett. **97**, 036401 (2006).
 - ⁴⁰ H. J. Schulz, Phys. Rev. Lett. **64**, 1445 (1990).
 - ⁴¹ M. Aichhorn, E. Arrigoni, M. Potthoff, and W. Hanke, Phys. Rev. B **74**, 024508 (2006).
 - ⁴² T. Giamarchi and C. Lhuillier, Phys. Rev. B **42**, 10641 (1990).
 - ⁴³ J. Reiss, D. Rohe, and W. Metzner, Phys. Rev. B **75**, 075110 (2007).
 - ⁴⁴ A. I. Lichtenstein and M. I. Katsnelson, Phys. Rev. B **62**, R9283 (2000).
 - ⁴⁵ T. Nakanishi, K. Yamaji, and T. Yanagisawa, Journal of the Physical Society of Japan **66**, 294 (1997).
 - ⁴⁶ M. Capone and G. Kotliar, Phys. Rev. B **74**, 054513 (2006).
 - ⁴⁷ X. Qian, J. Liu, L. Fu, and J. Li, Science **346**, 1344 (2014).
 - ⁴⁸ Z. Fei *et al.*, arXiv preprint arXiv:1610.07924 (2016).
 - ⁴⁹ F. Zheng *et al.*, Advanced Materials **28**, 4845 (2016).